



# Acute and Long-Term Circuit-Level Effects in the Auditory Cortex After Sound Trauma

Marcus Jeschke<sup>1,2,3,4\*†</sup>, Max F. K. Happel<sup>1,2,5†</sup>, Konstantin Tziridis<sup>6</sup>, Patrick Krauss<sup>6</sup>, Achim Schilling<sup>6</sup>, Holger Schulze<sup>6‡</sup> and Frank W. Ohl<sup>1,2,5\*‡</sup>

<sup>1</sup> Leibniz Institute for Neurobiology (LIN), Magdeburg, Germany, <sup>2</sup> Institute of Biology (IBIO), Otto-von-Guericke University Magdeburg (OVGU), Magdeburg, Germany, <sup>3</sup> Cognitive Hearing in Primates Group, Auditory Neuroscience and Optogenetics Laboratory, German Primate Center, Göttingen, Germany, <sup>4</sup> Institute for Auditory Neuroscience Göttingen, University Medical Center, Göttingen, Germany, <sup>5</sup> Center for Behavioral Brain Sciences (CBBS), Magdeburg, Germany, <sup>6</sup> Experimental Otolaryngology, Friedrich-Alexander University Erlangen-Nürnberg (FAU), Erlangen, Germany

## OPEN ACCESS

### Edited by:

Julio C. Hechavarría,  
Goethe University Frankfurt, Germany

### Reviewed by:

Alexander Galazyuk,  
Northeast Ohio Medical University,  
United States  
Ashley Lauren Schormans,  
Western University (Canada), Canada

### \*Correspondence:

Marcus Jeschke  
mjeschke@dpz.eu;  
marcus.jeschke@med.uni-  
goettingen.de  
Frank W. Ohl  
frank.ohl@lin-magdeburg.de

<sup>†</sup> These authors have contributed  
equally to this work and share first  
authorship

<sup>‡</sup> These authors have contributed  
equally to this work and share last  
authorship

### Specialty section:

This article was submitted to  
Auditory Cognitive Neuroscience,  
a section of the journal  
Frontiers in Neuroscience

**Received:** 24 August 2020

**Accepted:** 02 December 2020

**Published:** 05 January 2021

### Citation:

Jeschke M, Happel MFK,  
Tziridis K, Krauss P, Schilling A,  
Schulze H and Ohl FW (2021) Acute  
and Long-Term Circuit-Level Effects  
in the Auditory Cortex After Sound  
Trauma. *Front. Neurosci.* 14:598406.  
doi: 10.3389/fnins.2020.598406

Harmful environmental sounds are a prevailing source of chronic hearing impairments, including noise induced hearing loss, hyperacusis, or tinnitus. How these symptoms are related to pathophysiological damage to the sensory receptor epithelia and its effects along the auditory pathway, have been documented in numerous studies. An open question concerns the temporal evolution of maladaptive changes after damage and their manifestation in the balance of thalamocortical and corticocortical input to the auditory cortex (ACx). To address these issues, we investigated the loci of plastic reorganizations across the tonotopic axis of the auditory cortex of male Mongolian gerbils (*Meriones unguiculatus*) acutely after a sound trauma and after several weeks. We used a residual current-source density analysis to dissociate adaptations of intracolumnar input and horizontally relayed corticocortical input to synaptic populations across cortical layers in ACx. A pure tone-based sound trauma caused acute changes of subcortical inputs and corticocortical inputs at all tonotopic regions, particularly showing a broad reduction of tone-evoked inputs at tonotopic regions around the trauma frequency. At other cortical sites, the overall columnar activity acutely decreased, while relative contributions of lateral corticocortical inputs increased. After 4–6 weeks, cortical activity in response to the altered sensory inputs showed a general increase of local thalamocortical input reaching levels higher than before the trauma. Hence, our results suggest a detailed mechanism for overcompensation of altered frequency input in the auditory cortex that relies on a changing balance of thalamocortical and intracortical input and along the frequency gradient of the cortical tonotopic map.

**Keywords:** noise-induced hearing loss, auditory cortex, circuit level analysis, thalamocortical, corticocortical

## INTRODUCTION

Exposure to harmful environmental sound is a common cause for hearing impairments, including the development of noise-induced hearing loss (NIHL) (Eggermont, 2017a,b). Hearing loss has become increasingly prevalent over the last decades (Shargorodsky, 2010) and may further lead to hyperacusis, the increased loudness sensitivity to sounds, or tinnitus, the perception of phantom

sound/s in the absence of physical sound sources. Exposure to high sound levels can severely damage the peripheral sensory receptor epithelia within the cochlea. Cochlear damage causes altered auditory processing along the auditory pathway (for review see e.g., Gourévitch et al., 2014; Eggermont, 2017a). While sound-trauma related changes have been mostly described for auditory brain stem centers, compensatory and/or erroneous functional map plasticity in higher sensory brain areas, as for instance the auditory cortex have also been demonstrated (Resnik and Polley, 2017; Koops et al., 2020). Such maladaptive map plasticity has been proposed to underlie the development of tinnitus (Eggermont, 2003; Engineer et al., 2011), although this classical model of tinnitus development has been challenged by alternative models (Schaette and Kempster, 2006; Krauss et al., 2016; Miyakawa et al., 2019; Deng et al., 2020). In any case, plastic changes of the tonotopic organization of the auditory cortex (ACx) have been found after noise exposure in both humans and animals (Muhlnickel et al., 1998; Eggermont and Komiya, 2000; Dietrich et al., 2001; Noreña, 2005; Chen et al., 2016; Resnik and Polley, 2017). Whereas peripheral damage initially leads to reduced activity within the damaged region of the cochlea, increased activity has been described for several nuclei along the auditory pathway from the dorsal cochlear nucleus on (Kaltenbach et al., 1998, 2004; Kaltenbach and Afman, 2000; Brozoski et al., 2002; Zacharek et al., 2002; Sun et al., 2009; Holt et al., 2010; Wu et al., 2016) and was interpreted as a potential physiological correlate of tinnitus (e.g., Noreña and Eggermont, 2003; Engineer et al., 2011; Ahlf et al., 2012; Tziridis et al., 2015). These findings seem to suggest that reduced input within the peripherally deafferented frequency range is not only compensated along the auditory pathway, but eventually leads to hyperactivity in specific tonotopic regions within the auditory pathway. The hyperactivity might be explained by selective amplification of previously subthreshold cortical inputs (Irvine, 2018). Other models explain the subcortical enhancement of activations by means of homeostatic plasticity (Schaette and Kempster, 2006; Schaette and McAlpine, 2011; Resnik and Polley, 2017), stochastic resonance (Krauss et al., 2016), or overamplification in corticofugal projections (Asokan et al., 2018). In addition, recent studies in rats have demonstrated that while partial hearing loss affects even neighboring audiovisual cortical areas, the loss-induced central gain enhancement was more locally confined to auditory areas (Schormans et al., 2017, 2019). While these data principally demonstrate broad involvement of many nuclei along the auditory pathway as well as corticofugal projections in reflecting and compensating damage of the auditory periphery, relatively little is known about the convergent contribution of thalamocortical and intracortical inputs to these effects.

In previous studies we developed a method to dissociate the thalamocortical from intracortical contributions to cortical activity (Happel et al., 2010, 2014; Happel and Ohl, 2017). The method is based on the analysis of the residuum of the current-source density (CSD) reconstructed from measurements of the local field potential along linear electrode arrays penetrating the cortical layers perpendicular to the cortical surface. Using a combination of electrophysiological analysis, electrical

microstimulation and pharmacological blocking of intracortically transsynaptically relayed activity, we have demonstrated that a non-vanishing residuum of the CSD, i.e., a non-zero net current in a Gaussian cylinder surrounding the electrode array axis, predominantly results from extracellular currents relayed to the cylinder via the horizontal projection systems of intracortical connections. The method is highly sensitive and allows, for example, determining the tuning with stimulus frequency of the relative contributions of thalamocortically and intracortically relayed activity to a given tonotopic site in cortex. Here, we used this approach to investigate the temporal evolution of thalamocortically and intracortically relayed contributions following NIHL. While changes in spontaneous activity are often considered as potential correlates for tinnitus we here focused on sound evoked activity in order to further our understanding of the effects of sound trauma on auditory processing. Our data suggest that a pure tone-based sound trauma causes acute changes of subcortical inputs and corticocortical circuits at all tonotopic regions in auditory cortex. Long-lasting adaptive processes adjust cortical processing over weeks to the altered sensory inputs. A better understanding of the circuit mechanisms underlying this dynamic temporal process may provide new implications to ameliorate the effects of noise-induced hearing loss or its common perceptual symptom of chronic tinnitus.

## MATERIALS AND METHODS

Experiments were performed on 17 adult male Mongolian gerbils (*Meriones unguiculatus*) (age: 3–6 months, body weight: 70–120 g) anesthetized with ketamine-xylazine. All experimental procedures were approved by local authorities of the State of Saxony-Anhalt, Germany, and were in accordance with the international guidelines for care and use of animals in research as detailed by the NIH.

### Surgical Procedure

Anesthesia was induced by intraperitoneal infusion (0.06 ml/h) of 45% ketamine (50 mg/ml, Ratiopharm, Germany), 5% xylazine (Rompun, 2%, BayerVital, Germany) and 50% isotonic sodium chloride solution (154 mmol/l, Braun, Germany). Throughout the anesthetic procedures the animal's body temperature was maintained at 37°C by means of remote controlled heating pads. Anesthetic depth was tested periodically using the hind limb withdrawal reflex. To reduce tracheobronchial secretions Glycopyrrolate (Robinul, 0.02 ml SC) was used after surgery and prior to recording. To fixate the animal's head during auditory free field stimulation we glued two M3 standoffs onto the midline of the skull using light curing adhesive and composite (Plurabond One-SE and Plurafill Flow, Pluradent, Offenbach, Germany) as a base layer and dental acrylic to shape the skull implant. Next, access to the right ( $n = 2$ ) or bilateral ( $n = 15$ ) ACx was achieved by removing the temporal muscle, followed by a craniotomy overlying the ACx between the eye and ear. A stainless steel insect pin placed in the frontal bone with contact to the dura served as reference for electrophysiological recordings.

## Electrophysiological Recordings

After surgery and while remaining anesthetized throughout the recordings, animals were transferred into an electrically and acoustically shielded sound-proof chamber (IAC, Niederkrüchten, Germany). The animal's head was fixed in place facing a speaker (Tannoy arena satellite; distance: 1 m) by screwing the head cap to a custom-made head holder. Using vasculature landmarks (Thomas et al., 1993), laminar 32 channel silicon arrays (Type: A1 × 32–5 mm-50–413, Neuronex Technologies, United States) were slowly inserted orthogonally to the cortical surface into field AI of the ACx through small slits in the dura made by hypodermic needles. Typically we inserted a recording array in each hemisphere of an animal ( $n = 15$ ) or only in the right hemisphere ( $n = 2$ ). Hemispheric differences of the effects were not observed. After insertion, the tissue was allowed to settle for at least 20 min. Local field potential (LFP) responses to pure tones covering a frequency range from 0.5 to 32 kHz (half-octave or octave steps; 100 ms duration; at least 80 repetitions) at a sound level of 44 and 64 dB SPL were recorded (MAP system, Plexon Inc., United States) to determine the best frequency (BF) at the recording site. Next, responses to varying sound levels (covering –6 to 94 dB SPL in 10 dB steps) at several frequencies were recorded. These frequencies included the BF, the sound trauma frequency (2 kHz, see below), one frequency at least 1 octave below and above the trauma frequency. All sounds were generated in Matlab, converted to analog signals with a data acquisition card (NI PCI-BNC2110; National Instruments, Germany), fed through a programmable attenuator (g.PAH, Guger Technologies; Austria) and amplified by a wide-range audio amplifier (Thomas Tech Amp75). A measurement microphone and conditioning amplifier were used to calibrate acoustic stimuli (G.R.A.S. 26AM and B&K Nexus 2690-A, Bruel & Kjaer, Germany).

## Sound Trauma and Experimental Time Line

For sound trauma induction a sine wave generator (HP 33120A) generated a 2 kHz sine wave which was amplified by a power amplifier (Alesis RA150) and fed to a separate speaker (Canton XS.2) placed 20 cm in front of the animal. The stimulation lasted for 75 min and was performed under general anesthesia as described above. Sound level was calibrated for each trauma induction to a final level of 115 dB SPL as explained above. Such trauma has been shown to produce a mild to moderate hearing loss in the range of 20 to 40 dB around the trauma frequency (Ahlf et al., 2012). Sound evoked responses from field AI of the ACx were recorded immediately before and after sound trauma induction (**Figure 1A**) within the same recording session. Afterward, craniotomies were filled with antibiotic gel (K-Y jelly) and covered by dental cement. Animals were then allowed to recover and underwent a second, final, recording session 4–6 weeks later. Again, animals were anesthetized, the craniotomies reopened and animals were transferred to a sound proof chamber. Location of recording site during trauma induction and during the recovery measurement 4–6 weeks later was kept similar due to the vascularization pattern, which serves

as reliable landmark for the tonotopic gradient in gerbil ACx (Thomas et al., 1993; Schulze et al., 1997). Tonotopic gradients in auditory cortex are generally stable over weeks in untreated control animals, as others and own experiments have shown (Bieszczad and Weinberger, 2010; Guo et al., 2013; Zempeltzi et al., 2020).

## Data Analysis

Based on the second spatial derivative of the laminar LFP profiles recorded from the auditory cortex in response to pure tone stimulation (**Figure 1B**) we calculated one-dimensional current source density (CSD) distribution as:

$$-CSD \approx \frac{\delta^2 \Phi(z)}{\delta z^2} = \frac{\Phi(z + n\Delta z) - 2\Phi(z) + \Phi(z - n\Delta z)}{(n\Delta z)^2} \quad (1)$$

where  $\Phi$  is the field potential,  $z$  the spatial coordinate perpendicular to the cortical laminae,  $\Delta z$  the spatial sampling interval (50  $\mu\text{m}$ ) (Mitzdorf, 1985). LFP profiles were smoothed with a weighted average (Hamming window) of 5 channels (corresponding to a spatial filter kernel of 250  $\mu\text{m}$ ; linear extrapolation of 2 channels at boundaries; see Happel et al. (2010). CSD profiles reveal patterns of current influx (sinks) and efflux (sources). From single trial CSD profiles we computed the average rectified CSD (AvgRecCSD) to investigate the temporal pattern of the overall transmembrane current flow at the recorded site (Givre et al., 1994) as:

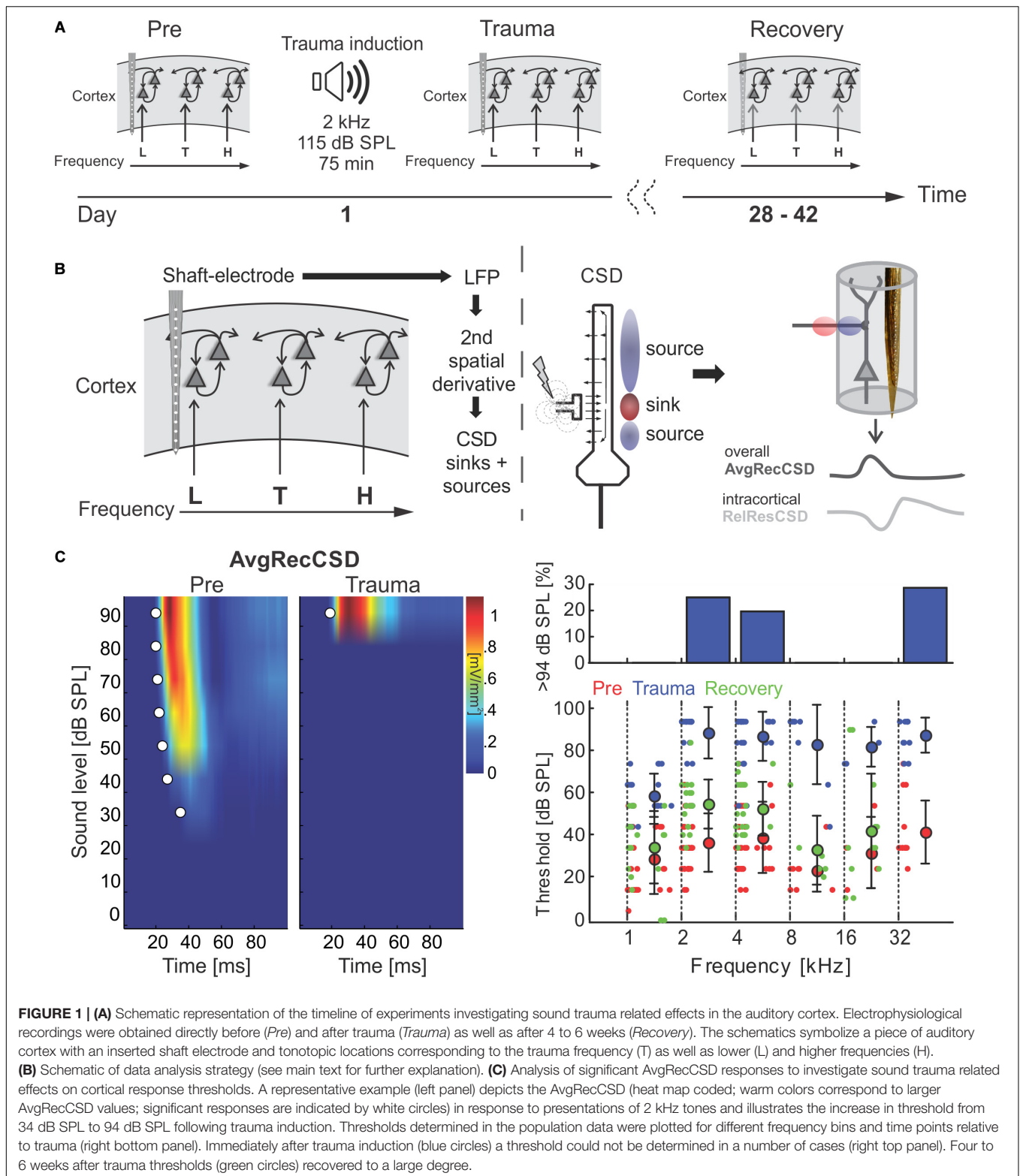
$$\text{AvgRecCSD} = \frac{\sum_{i=1}^n |CSD_i(t)|}{n} \quad (2)$$

The relative residue of the CSD (RelResCSD) is defined as the sum of the non-rectified magnitudes divided by the rectified magnitudes for each channel:

$$\text{RelResCSD} = \frac{\sum_{i=1}^n CSD_i(t)}{\sum_{i=1}^n |CSD_i(t)|} \quad (3)$$

Thereby, the RelResCSD quantifies the spatiotemporal ratio of unbalanced transmembrane charge transfer along the recording axis (Harding, 1992). We demonstrated before that the residual measure of the CSD thereby provides a quantitative measure of the lateral corticocortical contribution to stimulus related activity (Happel et al., 2010; Happel and Ohl, 2017).

The tonotopic region of the cortical patch under observation was characterized based on responses to varying pure tones covering a frequency range from 0.5 to 32 kHz at moderate sound levels (44 and 64 or 64 dB SPL). Based on the canonical CSD pattern we defined individual sink components in granular (S1), supragranular (S2) and early (iS1) and late (S3) infragranular layers, as explained in detail elsewhere (Happel et al., 2010; Schaefer et al., 2015; for an example, see **Figure 4A**). Peak amplitudes and onset latencies of individual current sinks were determined for individual channels and then averaged. Onset latencies were determined using a linear fit around the point where each curve surpasses 3 standard deviations above/below baseline (Happel et al., 2010). Frequencies evoking maximal responses of the granular sink were defined as the BF. Response threshold was determined as the lowest sound



intensity eliciting a significant response at any characteristic frequency 3 standard deviations over baseline (>5 ms). Response bandwidths were quantified as Q40dB-values 40 dB above response threshold.

For further quantitative analyses, we split the tonotopic axis into tonotopic regions below the trauma (0.5–<2 kHz), around the trauma (2–<8 kHz) and above the trauma (8–32 kHz). Thresholds for pure tone stimulation were calculated

based on sound intensity profiles of AvgRecCSD responses and were taken as the lowest sound level at which the root-mean-squared AvgRecCSD during stimulus presentation exceeded 3 standard deviations above prestimulus baseline levels. RelResCSD were considered if the AvgRecCSD response was found to be significant. The relationship between the overall strength of cortical activation and potential corticocortical contributions was investigated by correlating the AvgRecCSD and RelResCSD obtained from sound intensity profiles. The slope and offset of linear regression lines were then taken as indicators of corticocortical contribution to cortical activity at a given recording site. Specifically, a steeper slope hence indicates a higher corticocortical contribution with increasing overall activation. The offset, however, reveals the strength of corticocortical contribution at the minimal cortical activation.

## Statistical Analysis

To investigate potential associations between two variables a Pearson correlation analysis was performed. In order to further analyze the relationship between two variables and compare potential changes across experimental conditions linear regressions were calculated. Parameters of linear regressions were compared with general linear models with the factors experimental stage (*Pre, Trauma, Recovery*) and tonotopic region (*below trauma, trauma, above trauma*). For statistical comparison between two groups, we used paired-sample Student-*t*-tests. Comparison of multiple groups was performed by multi-factorial repeated measures ANOVAs (with Huynh-Feldt correction of sphericity) with a general significance level of  $\alpha = 0.05$ . For *post hoc* tests we used paired-sample Student-*t*-tests with Bonferroni-corrected levels of significance in case of testing repeatedly for  $n_{\text{test}}$  times of  $\alpha^* = \alpha/n_{\text{test}}$ . Due to the number of *post hoc* comparisons, we indicate significant differences of two subgroups with an asterisk within the corresponding figures. Comparisons without an asterisk were not significantly different.

## RESULTS

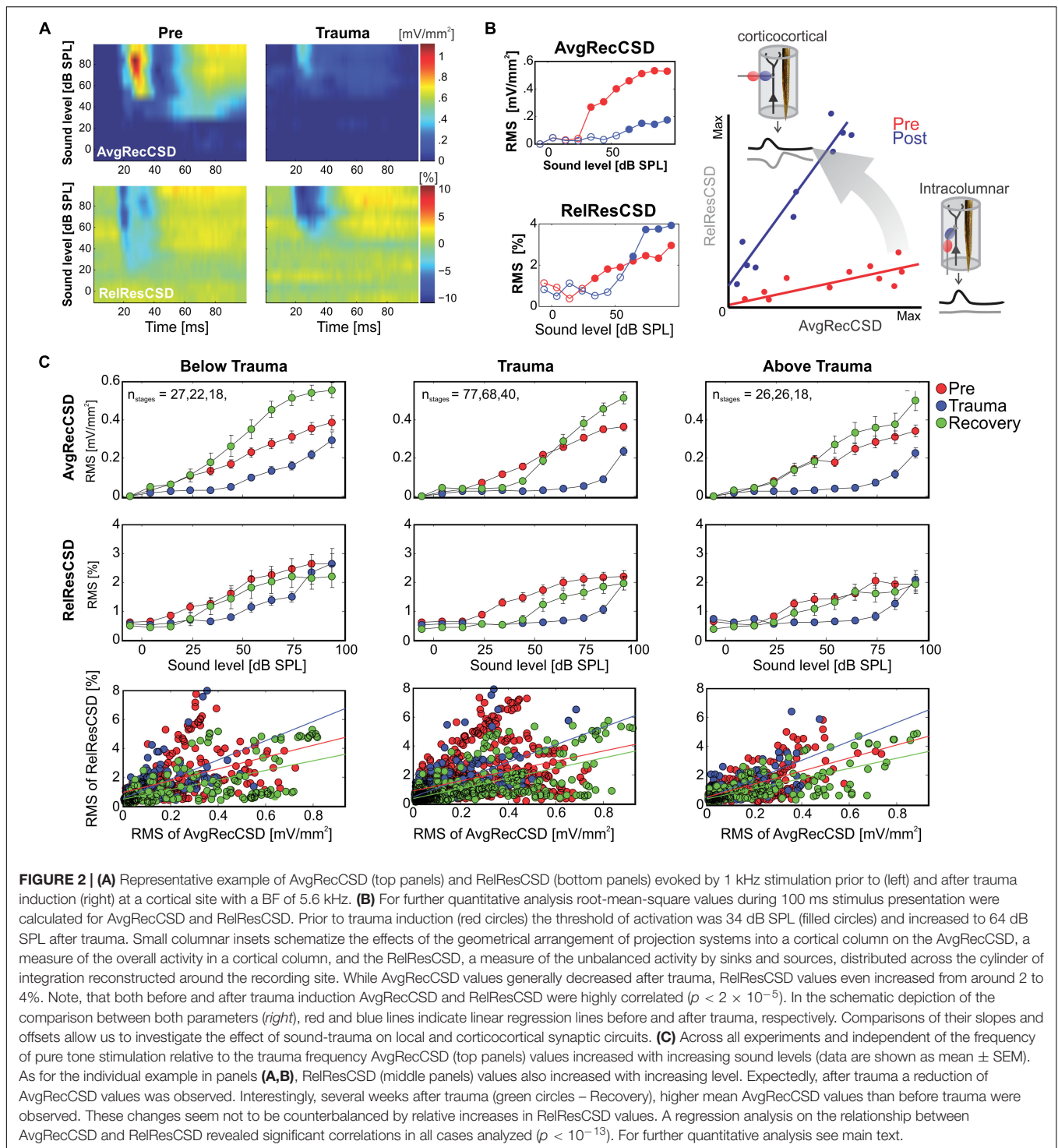
### Acoustic Trauma Led to Increases in Threshold of Cortical Activation

We here investigated the effect of a permanent mild to moderate sound-induced hearing loss on auditory cortical processing. To induce the acoustic trauma we employed a previously established procedure, presenting a 2 kHz pure tone at 115 dB SPL for 75 min (Ahlf et al., 2012). Using multichannel shaft electrode arrays, penetrating all cortical layers, electrophysiological recordings of local field potentials evoked by pure tones of varying frequency and intensity were performed immediately before and after trauma induction as well as after 4–6 weeks of recovery (Figure 1A). Across different animals we recorded from different frequency representations within the tonotopic map. From the local field potential data, current source density (CSD) profiles across the cortical laminae were reconstructed, and in addition averaged rectified CSDs (AvgRecCSD) and relative residuals (RelResCSD) were determined as measures of the overall cortical activity in a cylinder around the shaft

electrode and of the relative contribution of intracortically relayed horizontal input to this activation, respectively (for rationale see Happel et al., 2010; Figure 1B). Analysis of the cortical activation using pure-tone evoked responses (Figure 1C, left) revealed that at 2 kHz stimulation frequency (at which frequency the trauma was induced later on) thresholds prior to trauma induction were  $36.4 \pm 13.7$  dB SPL and increased to  $88.2 \pm 12.1$  dB SPL acutely after trauma resulting in an average increase in threshold of 51.8 dB (Figure 1C). However, this only serves as a lower estimate as we were not able to drive significant cortical activation at the highest sound level tested (94 dB SPL) in 25% of recordings (Figure 1C, upper right panel). Threshold increases were found throughout a large frequency region extending from at least 1 octave below and up to 4 octaves above the trauma frequency. At 1 kHz thresholds increased by an average of 30.1 dB from  $28.4 \pm 16.5$  dB. From 4 to 32 kHz thresholds increased on average by  $50.9 \pm 6.3$  dB. Even at a stimulation frequency of 32 kHz we were not able to determine a response threshold immediately after the trauma in 4 out of 14 cases. When tested after several weeks, thresholds recovered to a large extent but not completely. A two-way repeated measures ANOVA with factors “experimental time point” and “frequency bin” yielded a main effect for the “time point” (*Pre vs. Recovery*;  $F_{1,195} = 19.277$ ,  $p < 1.85 \times 10^{-5}$ ) such that average thresholds were  $45.13 \pm 18.6$  dB after recovery amounting to an average residual threshold increase of 10.1 dB. Additionally, the main effect of the factor “frequency bin” was also significant ( $F_{5,195} = 6.729$ ,  $p < 8.268 \times 10^{-6}$ ).

### Acute Increase of Corticocortical Activity After Sound Trauma and Long-Term Compensation

The relative weights of thalamocortically and intracortically relayed contributions to cortical plasticity following exposure to intense sounds are yet unclear. The analysis of the relative residues of the CSD allowed us to test whether the recruitment of corticocortical horizontal processes is altered following acoustic trauma. We followed the main hypothesis that after sound trauma the RelResCSD (which is mainly determined by intracortically, rather than thalamocortically, relayed inputs) is increased even though the overall cortical activation might be diminished. Figures 2A,B illustrate a representative example in which the overall cortical activation was decreased after trauma induction (1 kHz stimulation; BF of 5.6 kHz) while, in line with this hypothesis, the contribution of corticocortical horizontal input was increased. This can be further assessed by calculating the slope of the regression between the AvgRecCSD and the RelResCSD amplitudes which indicates how strongly corticocortical contributions increase with increasing overall activation (Figure 2B; right). We calculated the root mean square values during stimulus presentation for AvgRecCSD and RelResCSD to quantify our observations. Although the threshold of activation increased by 30 dB with an accompanying decrease of the strength of activation by 77%, the relative corticocortical contribution increased by  $\sim 10\%$ . Above threshold



this pattern remained: while the strength of activation was decreased (by 71–67% from 64 to 94 dB SPL) the relative corticocortical contribution consistently increased (by 51–33% from 64 to 94 dB SPL). Notably, as the strength of activation increased with increasing sound level, so did the corticocortical contribution. Consequently, the AvgRecCSD and RelResCSD were highly and significantly correlated before

( $R = 0.943$ ;  $p < 1.4 \times 10^{-5}$ ) and after trauma induction ( $R = 0.95$ ;  $p < 9 \times 10^{-6}$ ). Across all experiments (Figure 2C) and independent of the frequency of pure tone stimulation the overall strength of cortical activation (Figure 2C; top) increased with increasing sound level in all experimental phases (Pre, Trauma and Recovery). After trauma induction a reduction of cortical activation was observed consistent with

earlier observations of a reduced subcortical drive (Heeringa and van Dijk, 2016). Furthermore, the relative corticocortical contribution also increased with increasing level (Figure 2C; middle). However, several weeks after the trauma, stronger cortical activation than before trauma was observed, while the intracortical contribution did reach values as approximately before the trauma (although there were slight differences above and below trauma frequency regions, see below). Therefore, we conclude that plastic reorganizations over weeks seem to have compensated for the acute increased lateral, corticocortical spread of activity.

Since significant correlations ( $p < 10^{-13}$ ; Figure 2C; bottom) between the strength of cortical activation and corticocortical contributions were observed during all phases of the experiment, we did not directly compare the data before and after trauma induction. Instead, we performed a linear regression analysis between AvgRecCSD and RelResCSD values to reveal potential changes in the recruitment of corticocortical processes after sound trauma independent of the strength of cortical activation (Figure 2C). The slope of the linear regression between both measures, as indicator of the corticocortical contribution (see Figure 2B), was steeper immediately after trauma (blue), while similar slopes were observed between pre-trauma (red) and recovery (green; detailed statistical analysis in the next paragraph). In other words, immediately after trauma induction, corticocortically relayed synaptic activity contributed more to the overall activation strengths. This relative increase recovered over several weeks (Figure 2C bottom). In order to quantify these observations we fitted linear regression models to the AvgRecCSD and RelResCSD data to obtain measures of slope and offset of these regressions. The linear regression analysis indicated that the slope between AvgRecCSD and RelResCSD, i.e., the contribution of corticocortical activity to the overall cortical activity, is dependent on the experimental stage and

tonotopic region ( $R^2 = 0.08$ , adjusted  $R^2 = 0.07$ ,  $F_{4,297} = 6.491$ ,  $p < 5.1 \times 10^{-5}$ ). Profound inter-subject differences probably explain the remaining variability. A trend for increased slopes was observed immediately after trauma ( $\beta = 1.31$ ,  $p = 0.059$ ), whereas lower slopes were detected after several weeks of recovery ( $\beta = -2.04$ ,  $p = 0.008$ ). A trend was further found for increased slopes in the trauma region ( $\beta = 1.55$ ,  $p = 0.054$ ). For further details see Table 1. The offset between AvgRecCSD and RelResCSD also depended on experimental stage and tonotopic region ( $R^2 = 0.03$ , adjusted  $R^2 = 0.02$ ,  $F_{4,297} = 2.578$ ,  $p = 0.038$ ). The remaining variability is potentially explained by large differences between subjects. A trend for decreased offsets was observed immediately after trauma ( $\beta = -0.11$ ,  $p = 0.096$ ) as well as increased offsets in the region above the trauma ( $\beta = 0.17$ ,  $p = 0.008$ ). For further details see Table 2.

## Response Tuning Revealed Differences Between Acute and Long-Term Tonotopic Reorganization

We presented varying pure tone frequencies of moderate intensity (44 and 64 dB SPL) before and acutely after the sound trauma, and after 4–6 weeks of recovery. Thereby we characterized the frequency tuning of each individual recording position. In general, acutely after the trauma we found a prominent decrease of tuning width due to the vanished responses to the mid frequency range of 2–<8 kHz in all recordings. Even at recording positions within the tonotopic representation of the mid frequency range no responses could be measured acutely after the sound trauma. After weeks, mid frequency responses only partially recovered. Figure 3A shows a representative example with vanished responses after the trauma from 2 kHz (trauma frequency) upwards (including the BF) based

TABLE 1 | Linear regression of slope.

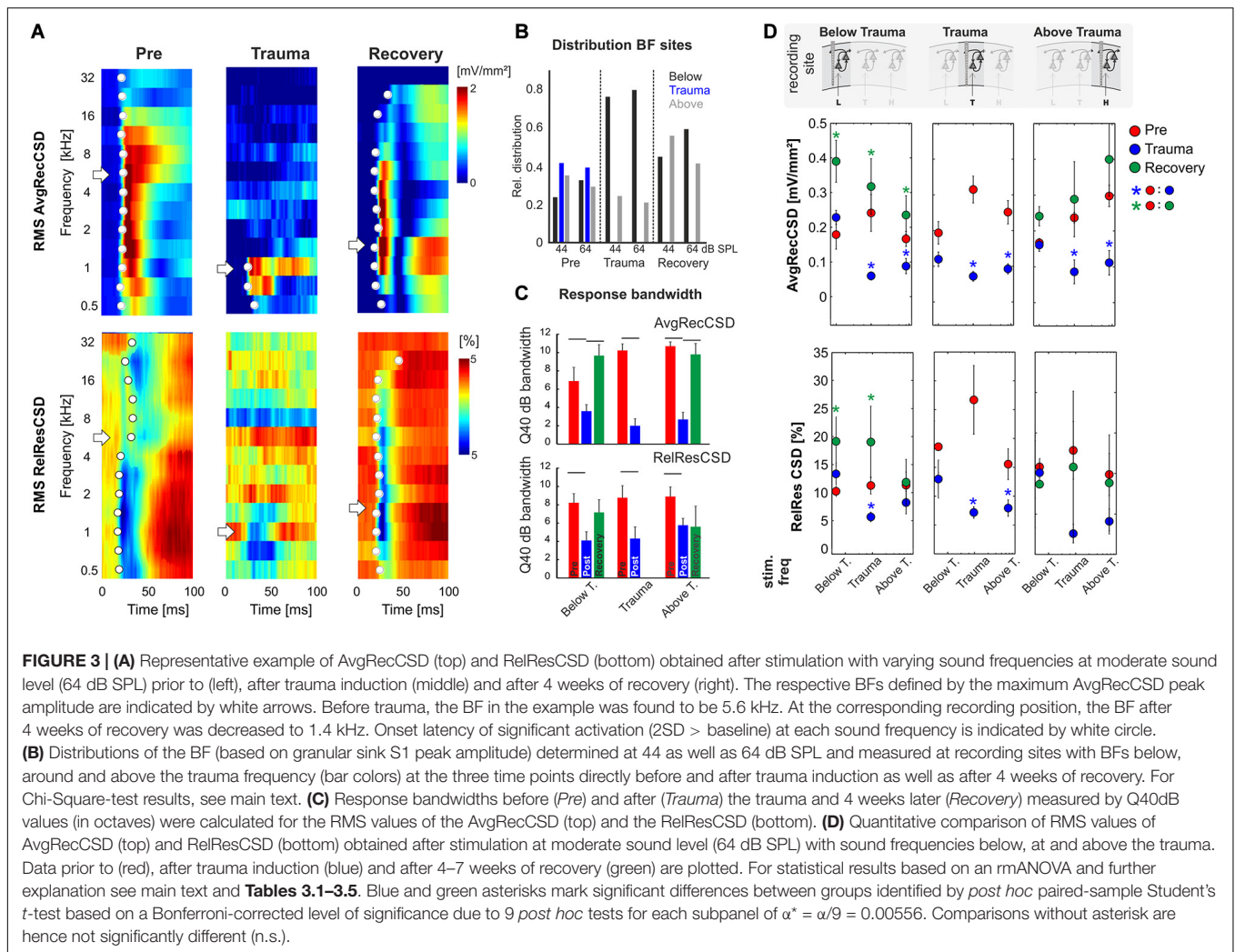
		$\beta$ Estimate	Std. Error	t value	Pr(> t )
Contrast to before trauma	(Intercept)	4.6706	0.6006	7.777	1.23e-13***
	Trauma	1.3112	0.6923	1.894	0.05921.
	Recovery	-2.0402	0.7644	-2.669	0.00803**
Contrast to below trauma region	Trauma	1.5460	0.7996	1.934	0.05411.
	Above	0.8681	0.6746	1.287	0.19915

Results from the linear regression analysis to test if the slope of the relationship between overall cortical activity and the relative contribution of corticocortical inputs depends on the experimental manipulation and tonotopic position. Significance codes: 0 "\*\*\*\*"; 0.001 "\*\*\*"; 0.05 ".".

TABLE 2 | Linear regression of offset.

		$\beta$ Estimate	Std. Error	t value	Pr(> t )
Contrast to before trauma	(Intercept)	0.55181	0.05748	9.601	<2e-16***
	Trauma	-0.11058	0.06626	-1.669	0.09617
	Recovery	-0.06962	0.07316	-0.952	0.34205
Contrast to below trauma region	Trauma	0.03474	0.07652	0.454	0.65012
	Above	0.17333	0.06456	2.685	0.00767**

Results from the linear regression analysis to test if the offset of the relationship between overall cortical activity and the relative contribution of corticocortical inputs depends on the experimental manipulation and tonotopic position. Significance codes: 0 "\*\*\*\*"; 0.001 "\*\*\*"; 0.05 ".".



on the RMS value of the AvgRecCSD (top). After weeks, tone-evoked RMS amplitudes of AvgRecCSD (top) and RelResCSD (bottom) largely recovered, even for the trauma frequency. Before trauma induction, BF sites were equally distributed across the frequency ranges below (<2 kHz), around (2–<8 kHz), and above (≥8 kHz) the trauma frequency for 44 dB SPL (*Pre*; Chi-square: 3.06, df: 2,  $p = 0.216$ ) and 64 dB SPL (Chi-square: 0.06, df: 2,  $p = 0.969$ ). After 4–6 weeks of recovery, we found significantly fewer sites with a BF in the range of 2–8 kHz with significant effects for stimulation with 64 dB SPL (*Recovery*; 64 dB SPL: Chi-square: 8.33, df: 2,  $p = 0.015$ ; 44 dB SPL: Chi-square: 0.115; df: 2,  $p = 0.11$ ; see **Figure 3A** for an example). Only in 1 individual example, the BF in the recovery measurement was in the range around trauma (2–8 kHz), which we therefore did not consider for statistical analyses (**Figure 3B**). For analyzing response bandwidths before (*Pre*) and after (*Trauma*) the trauma and 4–6 weeks later (*Recovery*), Q40dB values (in octaves) were calculated for the RMS value of the AvgRecCSD and RelResCSD. AvgRecCSD and RelResCSD response bandwidths showed significant reduction acutely after trauma induction in all 3 tonotopic site categories, viz. tonotopic regions with BFs

below, near and above the trauma frequency. A full recovery of response bandwidths was found at recording sites below or above the trauma after 4–6 weeks of recovery, but not at the trauma site (**Figure 3C**).

Based on the RMS values of AvgRecCSD and RelResCSD obtained after stimulation at a moderate sound level (64 dB SPL) evoked responses were divided into sound frequency bins below, at and above the trauma frequency (**Figure 3D**; note that we distinguish between *trauma site* which is the recording site at the tonotopic position of the trauma frequency (cf. the three columns of **Figure 3D**), and *trauma frequency* which is the stimulation frequency used to induce the trauma (cf. abscissa values in the graphs in each column of **Figure 3D**). After trauma induction, AvgRecCSD was significantly reduced for stimulation frequencies near and above the trauma frequency, but not below the trauma frequency, irrespective of the recording site. This is reflected by a 2-way rmANOVA for data obtained at each recording site that revealed main effects for the factor “stimulation frequency” and an interaction of factors “time point × stimulation frequency” for recording sites below the trauma, main effects for “frequency” at recording sites at the

trauma, and mainly interaction effects at sites above the trauma (Tables 3.1–1.3). *Post hoc* Bonferroni-corrected Student's *t*-tests were used to investigate statistical difference between paired samples. RelResCSD was most significantly reduced at the trauma site for frequencies near the trauma frequency (2-factorial rmANOVA with main effect of factor “stimulation frequency” (Table 1.5). After 4–6 weeks of recovery, AvgRecCSD and RelResCSD were significantly increased for most stimulation frequencies in tonotopic regions below the trauma (main effects for the factor “stimulation frequency” and an interaction of factors “time point × stimulation frequency”; Table 3.4). No significant changes of both parameters were found before the trauma and after 4–6 weeks at BF sites higher than the trauma indicating a full recovery (no sig. effects for the rmANOVA tested on the RelResCSD at BF high).

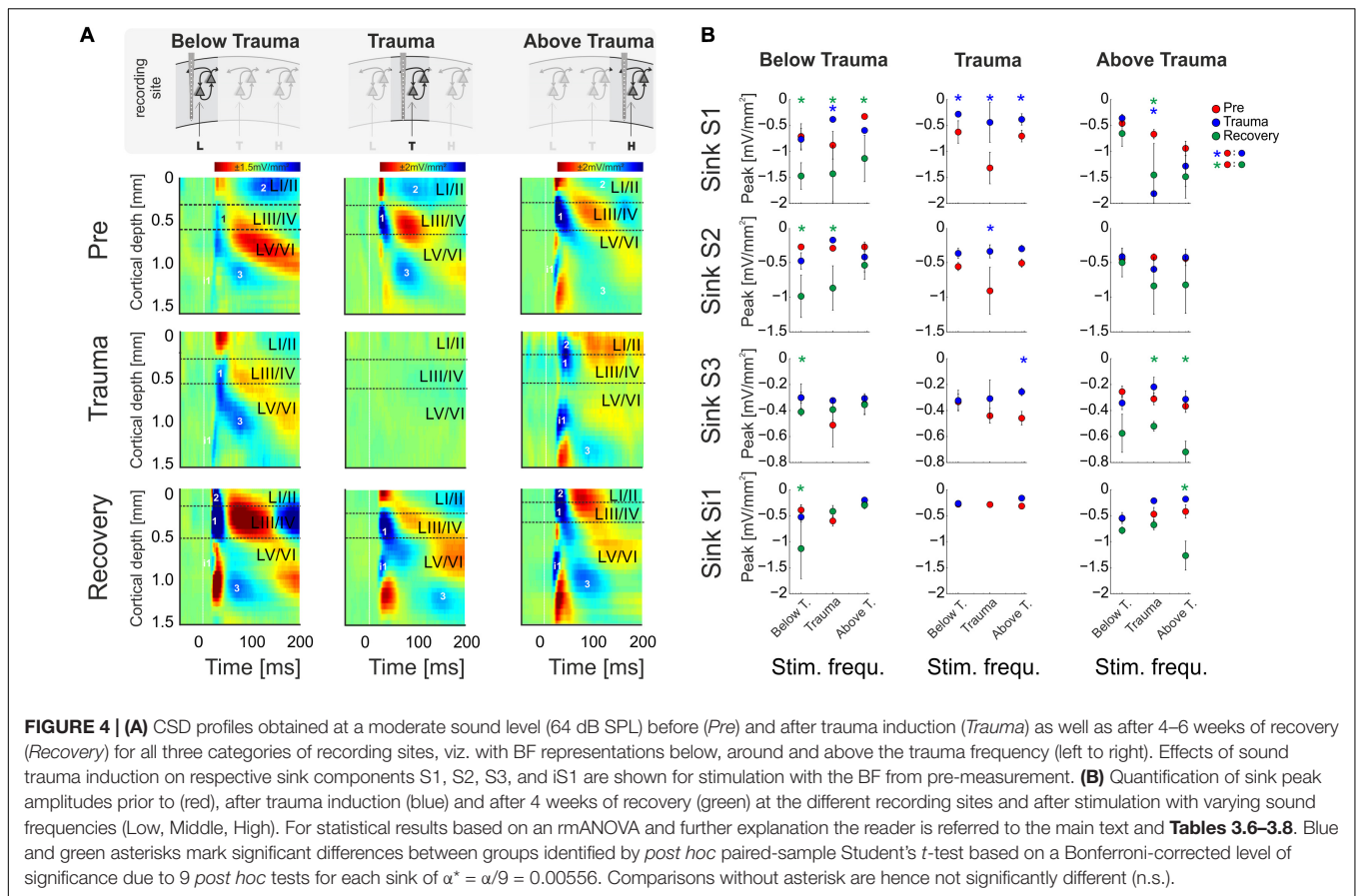
## Layer-Specific Changes of Synaptic Circuits Underlying Compensatory Tonotopic Shifts

In order to reveal layer-specific changes of synaptic processing in AI, CSD profiles at moderate sound level (64 dB SPL) were further analyzed directly before and after trauma induction as well as after 4–6 weeks. Figure 4A shows a representative example of effects of sound trauma induction on early sinks in granular layers III/IV (S1) and infragranular layers V (iS1), and subsequent

sinks in supragranular layers I/II (S2) and infragranular layers VI (S3). Within subjects, CSD profiles showed comparable BFs during the *pre/trauma* and *recovery* recordings at regions above and below the trauma. For recovery measurement in animals with recordings at BF sites around the trauma in the pre-condition, we compared cortical activity after stimulation with the BF measured before trauma induction (see above). Sinks S1 and iS1 are neuronal observables of early thalamocortical synaptic input and immediate local corticocortical amplification, while S2 and S3 are related to supragranular and infragranular corticocortical synaptic populations, respectively (Stoelzel et al., 2008; Happel et al., 2010; Schaefer et al., 2015). Below trauma (<2 kHz), the given example shows no significant change of the BF-evoked CSD profile after noise exposure, but a general increase of synaptic current flow across the entire cortical column after recovery. At tonotopic patches around the trauma site, we found a highly significant reduction of all early and late sink components after the noise trauma. After 4–6 weeks, cortical activation at these regions showed again a typical canonical feedforward CSD profile with initial input in granular (S1) and infragranular (iS1) layers and subsequent transaminar activations (S2 and S3). However, tonotopic tuning generally shifted its BF/CF tuning away from the initial BF range around the trauma frequency between 2 and 8 kHz (Figure 4B). At tonotopic sites above the trauma (>8 kHz), trauma induction did not lead to obvious immediate changes while stimulating with the BF. After the recovery a significant

**TABLE 3** | Report of significant repeated measures ANOVA effects for CSD parameters. rmANOVAs were Huyn-Feldt corrected and based on a significance level of  $\alpha^* = 0.05$ .

Factor	F-value	p-value
<b>1. Figure 3D; 2-way rmANOVA to test for AvgRecCSD RMS for “time point” and “frequency” at “Below Trauma” regions (2-way rmANOVA; <math>\alpha^* = 0.05</math>)</b>		
“stimulation frequency”	$F_{2,24} = 0.86$	$p < 0.001$
“stimulation frequency × time point”	$F_{4,48} = 4.62$	$p = 0.007$
<b>2. Figure 3D; 2-way rmANOVA to test for AvgRecCSD RMS for “time point” and “frequency” at “Trauma” regions (2-way rmANOVA; <math>\alpha^* = 0.05</math>)</b>		
“stimulation frequency”	$F_{2,24} = 25.59$	$p < 0.001$
<b>3. Figure 3D; 2-way rmANOVA to test for AvgRecCSD RMS for “time point” and “frequency” at “Above Trauma” regions (2-way rmANOVA; <math>\alpha^* = 0.05</math>)</b>		
“stimulation frequency × time point”	$F_{4,48} = 2.83$	$p = 0.042$
<b>4. Figure 3D; 2-way rmANOVA to test for RelRes RMS for “time point” and “frequency” at “Below Trauma” regions (2-way rmANOVA; <math>\alpha^* = 0.05</math>)</b>		
“stimulation frequency”	$F_{2,24} = 1.53$	$p = 0.016$
“stimulation frequency × time point”	$F_{4,48} = 3.28$	$p = 0.033$
<b>5. Figure 3D; 2-way rmANOVA to test for RelRes RMS for “time point” and “frequency” at “Trauma” regions (2-way rmANOVA; <math>\alpha^* = 0.05</math>)</b>		
“stimulation frequency”	$F_{2,24} = 21.91$	$p < 0.001$
<b>6. Figure 4B; 3-way rmANOVA to test for layer-specific tuning shifts at “Below Trauma” regions (3-way rmANOVA; <math>\alpha^* = 0.05</math>)</b>		
“Sink”	$F_{3,36} = 14.1$	$p < 0.001$
“stimulation Frequency”	$F_{2,24} = 10.6$	$p < 0.001$
“stimulation frequency × time point”	$F_{4,48} = 5.38$	$p = 0.0051$
“Sink × stimulation frequency”	$F_{6,72} = 3.53$	$p = 0.042$
“Sink × stimulation frequency × time point”	$F_{12,144} = 2.87$	$p = 0.046$
<b>7. Figure 4B; 3-way rmANOVA to test for layer-specific tuning shifts at “Trauma” regions (3-way rmANOVA; <math>\alpha^* = 0.05</math>)</b>		
“Time point”	$F_{2,24} = 3.47$	$p = 0.047$
“stimulation frequency”	$F_{2,24} = 3.74$	$p = 0.039$
“Sink × stimulation frequency × time point”	$F_{12,144} = 4.15$	$p = 0.007$
<b>8. Figure 4B; 3-way rmANOVA to test for layer-specific tuning shifts at “Above Trauma” regions (3-way rmANOVA; <math>\alpha^* = 0.05</math>)</b>		
“Sink”	$F_{2,30} = 55$	$p < 0.001$
“stimulation frequency × time point”	$F_{2,30} = 72.6$	$p < 0.001$



increase was observed mainly in early and late infragranular activity. Increased supragranular activation showed a similar trend as at sites with BFs below the trauma.

In order to quantify these circuit effects, we have analyzed sink peak amplitudes (**Figure 4**). Sink peak amplitudes at recording sites below the trauma showed no significant change after noise induction (compare with **Figure 3D**) except for a decreased granular sink amplitude for stimulation within the trauma frequency range. After recovery, at tonotopic regions below the trauma all four sink components were increased when stimulating with the BF (cf. frequency bin “Below T.”; 3-way rmANOVA with significant effects for main factor “sink,” but not for “time point” or “stimulation frequency”; **Table 3.6**). Therewith, the layer-specific sink activity adaptation is in accordance with the columnar AvgRecCSD response, which was also increased after recovery at tonotopic sites below the trauma for all stimulation frequencies (cf. **Figure 3D**). The subsequent CSD profile analysis revealed that this was due to significantly increased activation across all cortical layers for low frequency stimulation, and to mainly increased granular activation for high frequency stimulation (**Figure 4B**). At tonotopic sites around the trauma (2–<8 kHz) the sound trauma generally reduced all sink peak amplitudes irrespective of the stimulation frequency acutely and long-term. Depending on peak amplitudes before the trauma induction, this decrease was significant (3-way rmANOVA with main effect of factor “time point” and

“stimulation frequency” and their interaction with the factor “sink”; **Table 3.7**). For recovery measurements no data could be obtained as no BFs between 2 and 8 kHz were observed (cf. above). At tonotopic sites with higher BFs ( $\geq 8$  kHz), acutely after the trauma the granular sink interestingly showed an enhanced peak amplitude for stimulation within the trauma frequency range, in contrast to sites below the trauma. At both sides apart from the trauma region, we consistently found increased early infragranular input (iS1), which may reflect mainly local and BF-specific thalamocortical input. After recovery, early granular input was still significantly increased for middle frequency stimulation, but not for frequencies of the actual high-frequency BF-range. In contrast to “below trauma” sites, we only observed a trend of increased supragranular activation, but a significant increase of late infragranular activation (3-way rmANOVA with main effects of factor “sink” and interaction of “stimulation frequency  $\times$  time point”; **Table 3.8**).

## DISCUSSION

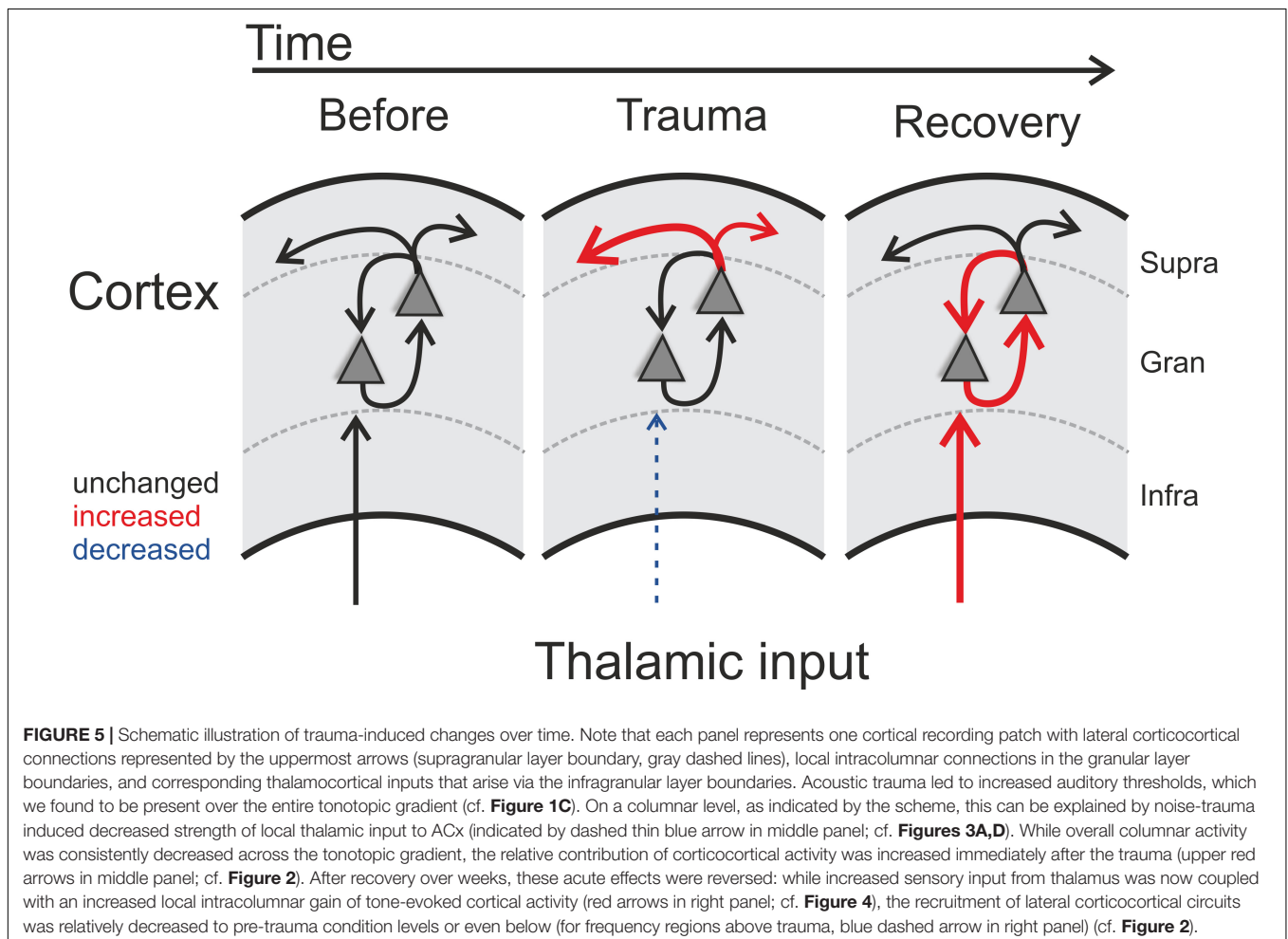
### Immediate Effects of Sound Trauma on Circuit-Level Activity in ACx

A huge body of literature has described neurophysiological changes throughout the auditory system following noise trauma

(for a review see e.g. Eggermont, 2017a). In this report we have described acute and long-term effects of noise trauma on functional neuronal circuitry in ACx with particular emphasis on the relative contributions of thalamocortically and intracortically relayed input to a tonotopic site. We demonstrated that exposing Mongolian gerbils to continuous, intense 2 kHz pure tones over 75 min led to increases in cortical activation thresholds across the hearing range of gerbils which recovered to a large extent over the course of 4–6 weeks leaving residual threshold increases of about 10 dB at the trauma frequency and slightly above (**Figure 1C**). Following such trauma, we found that acutely the overall activity within ACx decreased while the relative contribution of inter-columnar corticocortical inputs to this overall activity increased (**Figure 5**; middle panel). These observations are in line with the study by Novák et al. (2016) who reported increased activity of different types of inhibitory interneurons in layers II/III and IV of ACx immediately after trauma which in addition to the reduced thalamic input would explain the overall activity reduction after trauma. Furthermore, they described an unmasking of excitatory inputs confined to layer II/III which might explain the relative increase of inter-columnar contribution.

### Chronic Effects of Sound Trauma on Circuit-Level Activity in ACx

After recovery from trauma, the overall activity of the ACx increased again and actually reached levels higher than during pre-trauma conditions which has been discussed to be a physiological correlate of subjective tinnitus (Noreña and Eggermont, 2003; Eggermont and Roberts, 2004; but see Miyakawa et al., 2019), while the relative contribution of corticocortical inputs decreased to levels even below (for frequency regions above trauma) or equal to pre-trauma conditions (**Figures 2, 3**). This finding leads to the conclusion that the high overall activity in ACx after recovery must result from a restored or even increased thalamic activation (**Figure 5**; right panel) which is in line with the increased activity in the medial geniculate body (MGB) reported after noise exposure (Kalappa et al., 2014). It seems likely that increased thalamic activation of ACx is the result of mechanisms of compensatory, homeostatic plasticity (Mosso et al., 2000; Schaette and Kempner, 2006; Noreña, 2011; Tighilet et al., 2016), stochastic resonance (Krauss et al., 2016, 2018) or modulation of corticofugal activity (Asokan et al., 2018). This conclusion is further supported by our layer-specific analysis,



demonstrating that early sink activity in both thalamocortical-recipient layers III/IV and Vb/VIa was significantly increased after recovery (**Figure 4B**). However, the increased gain was limited to local intracolumnar circuits and was not broadcast to wide-spread corticocortical circuits (cf. Schormans et al., 2019). This seems in line with earlier observations which demonstrated that higher activity after noise trauma and also after salicylate-induced hearing loss was restricted to regions with changed tonotopy (Seki and Eggermont, 2003; Stolzberg et al., 2012). Our results suggest an overcompensation of altered frequency input in auditory cortex that is limited to local circuits which might impact on crosscolumnar spectral integration across the tonotopic gradient (for a schematic summary of our findings refer to **Figure 5**).

## Plasticity in Local Cortical Circuits and Their Long Term Compensation

In order to reveal frequency tuning changes across ACx, we analyzed the trauma induced plasticity of tuning functions at different tonotopic regions and revealed specific effects in relation to the trauma frequency. Specifically, we found a stronger overall cortical activation several weeks after the trauma at tonotopic sites with BF representations lower than the trauma frequency (**Figure 3D**; top left) which was accompanied by an increase of the relative residual CSD (**Figure 3D**; bottom left). At tonotopic high-frequency regions, overall columnar activation was moderately increased irrespective of the stimulation frequency (**Figure 3D**; top right), without an increase of relative corticocortical contributions (**Figure 3D**; bottom left) in line with the aforementioned overcompensation (**Figure 2**). The trauma frequency-dependent effects described are highly likely to be related to the frequency-specific noise exposure, as tonotopic gradients in untreated control animals are generally stable over weeks (Ohl et al., 2001; Bieszczad and Weinberger, 2010; Guo et al., 2013; Happel et al., 2014; Deliano et al., 2020; Zempeltzi et al., 2020).

The quantitative analysis of the individual sink components further showed that this increase in spectral representation at tonotopic sites below the trauma was mediated mainly by synaptic inputs in granular layers (S1) and corticocortical inputs in supragranular layers (S2). Thalamocortical inputs in infragranular layers (iS1) were only increased for BF stimulation (**Figure 4B**; left column). Such a significant increase of broad spectral input in granular and supragranular layers was absent at tonotopic regions above the trauma (**Figure 4B**; right column). Nevertheless, in regions below the trauma early infragranular sink activity was significantly enhanced for BF-stimulation. This difference of early inputs in granular and infragranular layers might indicate a differential sound trauma sensitivity of the tuning width for thalamocortical inputs in granular layers and collaterals in deeper layers yielding different contributions to cortical tuning (Constantinople and Bruno, 2013). Interestingly, the observation of a reduction of perineuronal nets in mice AI after acoustic trauma (Nguyen et al., 2017) may be a prerequisite for all the chronic plastic changes described in our report as they presumably require adaptations in synaptic connectivity.

Considering our finding of compensated (below trauma) or even overcompensated (above trauma) relative contributions of lateral input, the described long-term effects on cortical frequency tuning might underlie a mainly local regulation of intracortical gain of afferent synaptic activity compensating the acute increase of relative crosscolumnar activity (cf. Schormans et al., 2019).

In summary, this study has demonstrated that pure-tone-induced sound trauma does not only alter net cortical activation, but leads to a change in the relative contributions of thalamocortically relayed and intracortically relayed activity. The reduction of cortical response amplitudes to pure-tone stimulation seen directly after trauma induction is accompanied by an acutely increased contribution of intracortically relayed input. After several weeks of recovery, when thalamic input tuned to the trauma frequency is increased again, the relative contribution of intracortically relayed input is decreased, at least to levels found before trauma induction.

## DATA AVAILABILITY STATEMENT

The data supporting the conclusions of this article will be made available on reasonable request to the corresponding authors.

## ETHICS STATEMENT

The animal study was reviewed and approved by Landesverwaltungsamt Sachsen-Anhalt, Referat 203 Verbraucherschutz, Veterinärangelegenheiten.

## AUTHOR CONTRIBUTIONS

MJ, MH, HS, and FO designed the research. MJ and MH performed all the experiments and analyzed the data. KT provided the new reagents and tools. All authors discussed the data, prepared the figures, and wrote the manuscript.

## FUNDING

This work was supported by grants from the Deutsche Forschungsgemeinschaft (DFG, SFB-TRR 31, TP A03) to FO and (DFG SCHU 1272/12-1) to HS. The funders had no role in study design, data collection and analysis, decision to publish, or preparation of the manuscript.

## ACKNOWLEDGMENTS

We thank Kathrin Ohl for technical assistance. This manuscript has been released as a pre-print at bioRxiv.org (Jeschke et al., 2020).

## REFERENCES

- Ahlf, S., Tziridis, K., Korn, S., Strohmeyer, I., and Schulze, H. (2012). Predisposition for and prevention of subjective tinnitus development. *PLoS ONE* 7:e44519. doi: 10.1371/journal.pone.0044519
- Asokan, M. M., Williamson, R. S., Hancock, K. E., and Polley, D. B. (2018). Sensory overamplification in layer 5 auditory corticofugal projection neurons following cochlear nerve synaptic damage. *Nat. Commun.* 9:2468. doi: 10.1038/s41467-018-04852-y
- Bieszczad, K. M., and Weinberger, N. M. (2010). Remodeling the cortex in memory: Increased use of a learning strategy increases the representational area of relevant acoustic cues. *Neurobiol. Learn. Mem.* 94, 127–144. doi: 10.1016/j.nlm.2010.04.009
- Brozoski, T. J., Bauer, C. A., and Caspary, D. M. (2002). Elevated fusiform cell activity in the dorsal cochlear nucleus of chinchillas with psychophysical evidence of tinnitus. *J. Neurosci.* 22, 2383–2390. doi: 10.1523/JNEUROSCI.22-06-02383.2002
- Chen, G.-D., Sheppard, A., and Salvi, R. (2016). Noise trauma induced plastic changes in brain regions outside the classical auditory pathway. *Neuroscience* 315, 228–245. doi: 10.1016/j.neuroscience.2015.12.005
- Constantinople, C. M., and Bruno, R. M. (2013). Deep cortical layers are activated directly by thalamus. *Science* 340, 1591–1594. doi: 10.1126/science.1236425
- Deliano, M., Brunk, M. G. K., El-Tabbal, M., Zempeltzi, M. M., Happel, M. F. K., and Ohl, F. W. (2020). Dopaminergic neuromodulation of high gamma stimulus phase-locking in gerbil primary auditory cortex mediated by D1/D5-receptors. *Eur. J. Neurosci.* 51, 1315–1327. doi: 10.1111/ejn.13898
- Deng, D., Masri, S., Yao, L., Ma, X., Cao, X., Yang, S., et al. (2020). Increasing endogenous activity of NMDARs on GABAergic neurons increases inhibition, alters sensory processing and prevents noise-induced tinnitus. *Sci. Rep.* 10:11969. doi: 10.1038/s41598-020-68652-5
- Dietrich, V., Nieschalk, M., Stoll, W., Rajan, R., and Pantev, C. (2001). Cortical reorganization in patients with high frequency cochlear hearing loss. *Hear. Res.* 158, 95–101. doi: 10.1016/S0378-5955(01)00282-9
- Eggermont, J. J. (2003). Central tinnitus. *Auris. Nasus. Larynx* 30, 7–12. doi: 10.1016/S0385-8146(02)00122-0
- Eggermont, J. J. (2017a). Acquired hearing loss and brain plasticity. *Hear. Res.* 343, 176–190. doi: 10.1016/j.heares.2016.05.008
- Eggermont, J. J. (2017b). Effects of long-term non-traumatic noise exposure on the adult central auditory system. Hearing problems without hearing loss. *Hear. Res.* 352, 12–22. doi: 10.1016/j.heares.2016.10.015
- Eggermont, J. J., and Komiya, H. (2000). Moderate noise trauma in juvenile cats results in profound cortical topographic map changes in adulthood. *Hear. Res.* 142, 89–101. doi: 10.1016/S0378-5955(00)00024-1
- Eggermont, J. J., and Roberts, L. E. (2004). The neuroscience of tinnitus. *Trends Neurosci.* 27, 676–682. doi: 10.1016/j.tins.2004.08.010
- Engineer, N. D., Riley, J. R., Seale, J. D., Vrana, W. A., Shetake, J. A., Sudanagunta, S. P., et al. (2011). Reversing pathological neural activity using targeted plasticity. *Nature* 470, 101–104. doi: 10.1038/nature09656
- Givre, S. J., Schroeder, C. E., and Arezzo, J. C. (1994). Contribution of extrastriate area V4 to the surface-recorded flash VEP in the awake macaque. *Vis. Res.* 34, 415–428. doi: 10.1016/0042-6989(94)90156-2
- Gourévitch, B., Edeline, J.-M., Ocellini, F., and Eggermont, J. J. (2014). Is the din really harmless? Long-term effects of non-traumatic noise on the adult auditory system. *Nat. Rev. Neurosci.* 15, 483–491. doi: 10.1038/nrn3744
- Guo, F., Intskirveli, I., Blake, D. T., and Metherate, R. (2013). Tone-detection training enhances spectral integration mediated by intracortical pathways in primary auditory cortex. *Neurobiol. Learn. Mem.* 101, 75–84. doi: 10.1016/j.nlm.2013.01.006
- Happel, M. F. K., Deliano, M., Handschuh, J., and Ohl, F. W. (2014). Dopamine-modulated recurrent corticoafferent feedback in primary sensory cortex promotes detection of behaviorally relevant stimuli. *J. Neurosci.* 34, 1234–1247. doi: 10.1523/JNEUROSCI.1990-13.2014
- Happel, M. F. K., Jeschke, M., and Ohl, F. W. (2010). Spectral integration in primary auditory cortex attributable to temporally precise convergence of thalamocortical and intracortical input. *J. Neurosci.* 30, 11114–11127. doi: 10.1523/JNEUROSCI.0689-10.2010
- Happel, M. F. K., and Ohl, F. W. (2017). Compensating level-dependent frequency representation in auditory cortex by synaptic integration of corticocortical input. *PLoS ONE* 12:e0169461. doi: 10.1371/journal.pone.0169461
- Harding, G. W. (1992). The currents that flow in the somatosensory cortex during the direct cortical response. *Exp. Brain Res.* 90, 29–39.
- Heeringa, A. N., and van Dijk, P. (2016). The immediate effects of acoustic trauma on excitation and inhibition in the inferior colliculus: a wiener-kernel analysis. *Hear. Res.* 331, 47–56. doi: 10.1016/j.heares.2015.10.007
- Holt, A. G., Bissig, D., Mirza, N., Rajah, G., and Berkowitz, B. (2010). Evidence of key tinnitus-related brain regions documented by a unique combination of manganese-enhanced MRI and acoustic startle reflex testing. *PLoS ONE* 5:e14260. doi: 10.1371/journal.pone.0014260
- Irvine, D. R. F. (2018). Plasticity in the auditory system. *Hear. Res.* 362, 61–73. doi: 10.1016/j.heares.2017.10.011
- Jeschke, M., Happel, M. F. K., Tziridis, K., Krauss, P., Schilling, A., Schulze, H., et al. (2020). Acute and long-term circuit-level effects in the auditory cortex after sound trauma. *bioRxiv* 2020:980730. doi: 10.1101/2020.03.06.980730
- Kalappa, B. I., Brozoski, T. J., Turner, J. G., and Caspary, D. M. (2014). Single unit hyperactivity and bursting in the auditory thalamus of awake rats directly correlates with behavioural evidence of tinnitus. *J. Physiol.* 592, 5065–5078. doi: 10.1113/jphysiol.2014.278572
- Kaltenbach, J. A., and Afman, C. E. (2000). Hyperactivity in the dorsal cochlear nucleus after intense sound exposure and its resemblance to tone-evoked activity: a physiological model for tinnitus. *Hear. Res.* 140, 165–172. doi: 10.1016/S0378-5955(99)00197-5
- Kaltenbach, J. A., Godfrey, D. A., Neumann, J. B., McCaslin, D. L., Afman, C. E., and Zhang, J. (1998). Changes in spontaneous neural activity in the dorsal cochlear nucleus following exposure to intense sound: relation to threshold shift. *Hear. Res.* 124, 78–84. doi: 10.1016/S0378-5955(98)00119-1
- Kaltenbach, J. A., Zacharek, M. A., Zhang, J., and Frederick, S. (2004). Activity in the dorsal cochlear nucleus of hamsters previously tested for tinnitus following intense tone exposure. *Neurosci. Lett.* 355, 121–125. doi: 10.1016/j.neulet.2003.10.038
- Koops, E. A., Renken, R. J., Lanting, C. P., and van Dijk, P. (2020). Cortical tonotopic map changes in humans are larger in hearing loss than in additional tinnitus. *J. Neurosci.* 40, 3178–3185. doi: 10.1523/JNEUROSCI.2083-19.2020
- Krauss, P., Tziridis, K., Metzner, C., Schilling, A., Hoppe, U., and Schulze, H. (2016). Stochastic resonance controlled upregulation of internal noise after hearing loss as a putative cause of tinnitus-related neuronal hyperactivity. *Front. Neurosci.* 10:597. doi: 10.3389/fnins.2016.00597
- Krauss, P., Tziridis, K., Schilling, A., and Schulze, H. (2018). Cross-modal stochastic resonance as a universal principle to enhance sensory processing. *Front. Neurosci.* 12:578. doi: 10.3389/fnins.2018.00578
- Mitzdorf, U. (1985). Current source-density method and application in cat cerebral cortex: investigation of evoked potentials and EEG phenomena. *Physiol. Rev.* 65, 37–100. doi: 10.1152/physrev.1985.65.1.37
- Miyakawa, A., Wang, W., Cho, S.-J., Li, D., Yang, S., and Bao, S. (2019). Tinnitus correlates with downregulation of cortical glutamate decarboxylase 65 expression but not auditory cortical map reorganization. *J. Neurosci.* 39, 9989–10001. doi: 10.1523/JNEUROSCI.1117-19.2019
- Mossop, J. E., Wilson, M. J., Caspary, D. M., and Moore, D. R. (2000). Down-regulation of inhibition following unilateral deafening. *Hear. Res.* 147, 183–187. doi: 10.1016/S0378-5955(00)00054-X
- Muhlcnickel, W., Elbert, T., Taub, E., and Flor, H. (1998). Reorganization of auditory cortex in tinnitus. *Proc. Natl. Acad. Sci.* 95, 10340–10343. doi: 10.1073/pnas.95.17.10340
- Nguyen, A., Khaleel, H. M., and Razak, K. A. (2017). Effects of noise-induced hearing loss on parvalbumin and perineuronal net expression in the mouse primary auditory cortex. *Hear. Res.* 350, 82–90. doi: 10.1016/j.heares.2017.04.015
- Noreña, A. J. (2005). Enriched acoustic environment after noise trauma reduces hearing loss and prevents cortical map reorganization. *J. Neurosci.* 25, 699–705. doi: 10.1523/JNEUROSCI.2226-04.2005
- Noreña, A. J. (2011). An integrative model of tinnitus based on a central gain controlling neural sensitivity. *Neurosci. Biobehav. Rev.* 35, 1089–1109. doi: 10.1016/j.neubiorev.2010.11.003

- Noreña, A. J., and Eggermont, J. J. (2003). Changes in spontaneous neural activity immediately after an acoustic trauma: implications for neural correlates of tinnitus. *Hear. Res.* 183, 137–153. doi: 10.1016/S0378-5955(03)00225-9
- Novák, O., Zelenka, O., Hromádka, T., and Syka, J. (2016). Immediate manifestation of acoustic trauma in the auditory cortex is layer specific and cell type dependent. *J. Neurophysiol.* 115, 1860–1874. doi: 10.1152/jn.00810.2015
- Ohl, F. W., Scheich, H., and Freeman, W. J. (2001). Change in pattern of ongoing cortical activity with auditory category learning. *Nature* 412, 733–736. doi: 10.1038/35089076
- Resnik, J., and Polley, D. B. (2017). Fast-spiking GABA circuit dynamics in the auditory cortex predict recovery of sensory processing following peripheral nerve damage. *eLife* 6:e21452. doi: 10.7554/eLife.21452
- Schaefer, M. K., Hechavarría, J. C., and Kössl, M. (2015). Quantification of mid and late evoked sinks in laminar current source density profiles of columns in the primary auditory cortex. *Front. Neural Circuits* 9:52. doi: 10.3389/fncir.2015.00052
- Schaette, R., and Kempter, R. (2006). Development of tinnitus-related neuronal hyperactivity through homeostatic plasticity after hearing loss: a computational model. *Eur. J. Neurosci.* 23, 3124–3138. doi: 10.1111/j.1460-9568.2006.04774.x
- Schaette, R., and McAlpine, D. (2011). Tinnitus with a normal audiogram: physiological evidence for hidden hearing loss and computational model. *J. Neurosci.* 31, 13452–13457. doi: 10.1523/JNEUROSCI.2156-11.2011
- Schormans, A. L., Typlt, M., and Allman, B. L. (2017). Crossmodal plasticity in auditory, visual and multisensory cortical areas following noise-induced hearing loss in adulthood. *Hear. Res.* 343, 92–107. doi: 10.1016/j.heares.2016.06.017
- Schormans, A. L., Typlt, M., and Allman, B. L. (2019). Adult-onset hearing impairment induces layer-specific cortical reorganization: evidence of crossmodal plasticity and central gain enhancement. *Cereb. Cortex* 29, 1875–1888. doi: 10.1093/cercor/bhy067
- Schulze, H., Ohl, F. W., Heil, P., and Scheich, H. (1997). Field-specific responses in the auditory cortex of the unanaesthetized mongolian gerbil to tones and slow frequency modulations. *J. Comp. Physiol. Neuroethol. Sens. Neural. Behav. Physiol.* 181, 573–589. doi: 10.1007/s003590050141
- Seki, S., and Eggermont, J. J. (2003). Changes in spontaneous firing rate and neural synchrony in cat primary auditory cortex after localized tone-induced hearing loss. *Hear. Res.* 180, 28–38. doi: 10.1016/S0378-5955(03)00074-1
- Shargorodsky, J. (2010). Change in prevalence of hearing loss in US adolescents. *JAMA* 304:772. doi: 10.1001/jama.2010.1124
- Stoelzel, C. R., Bereshpolova, Y., Gusev, A. G., and Swadlow, H. A. (2008). The impact of an LGNd impulse on the awake visual cortex: Synaptic dynamics and the sustained/transient distinction. *J. Neurosci.* 28, 5018–5028. doi: 10.1523/JNEUROSCI.4726-07.2008
- Stolzberg, D., Chrostowski, M., Salvi, R. J., and Allman, B. L. (2012). Intracortical circuits amplify sound-evoked activity in primary auditory cortex following systemic injection of salicylate in the rat. *J. Neurophysiol.* 108, 200–214. doi: 10.1152/jn.00946.2011
- Sun, W., Lu, J., Stolzberg, D., Gray, L., Deng, A., Lobarinas, E., et al. (2009). Salicylate increases the gain of the central auditory system. *Neuroscience* 159, 325–334. doi: 10.1016/j.neuroscience.2008.12.024
- Thomas, H., Tillein, J., Heil, P., and Scheich, H. (1993). Functional organization of auditory cortex in the mongolian gerbil (*Meriones unguiculatus*). I. Electrophysiological mapping of frequency representation and distinction of fields. *Eur. J. Neurosci.* 5, 882–897. doi: 10.1111/j.1460-9568.1993.tb00940.x
- Tighilet, B., Duthheil, S., Siponen, M. I., and Noreña, A. J. (2016). Reactive neurogenesis and down-regulation of the potassium-chloride cotransporter KCC2 in the cochlear nuclei after cochlear deafferentation. *Front. Pharmacol.* 7:281. doi: 10.3389/fphar.2016.00281
- Tziridis, K., Ahlf, S., Jeschke, M., Happel, M. F. K., Ohl, F. W., and Schulze, H. (2015). Noise trauma induced neural plasticity throughout the auditory system of Mongolian gerbils: differences between tinnitus developing and non-developing animals. *Front. Neurol.* 6:22. doi: 10.3389/fneur.2015.00022
- Wu, C., Stefanescu, R. A., Martel, D. T., and Shore, S. E. (2016). Tinnitus: maladaptive auditory–somatosensory plasticity. *Hear. Res.* 334, 20–29. doi: 10.1016/j.heares.2015.06.005
- Zacharek, M. A., Kaltenbach, J. A., Mathog, T. A., and Zhang, J. (2002). Effects of cochlear ablation on noise induced hyperactivity in the hamster dorsal cochlear nucleus: implications for the origin of noise induced tinnitus. *Hear. Res.* 172, 137–144. doi: 10.1016/S0378-5955(02)00575-0
- Zempeltzi, M. M., Kisse, M., Brunk, M. G. K., Glemser, C., Aksit, S., Deane, K. E., et al. (2020). Task rule and choice are reflected by layer-specific processing in rodent auditory cortical microcircuits. *Commun. Biol.* 3:345. doi: 10.1038/s42003-020-1073-3

**Conflict of Interest:** The authors declare that the research was conducted in the absence of any commercial or financial relationships that could be construed as a potential conflict of interest.

Copyright © 2021 Jeschke, Happel, Tziridis, Krauss, Schilling, Schulze and Ohl. This is an open-access article distributed under the terms of the Creative Commons Attribution License (CC BY). The use, distribution or reproduction in other forums is permitted, provided the original author(s) and the copyright owner(s) are credited and that the original publication in this journal is cited, in accordance with accepted academic practice. No use, distribution or reproduction is permitted which does not comply with these terms.